Biochimica et Biophysica Acta, 1057 (1991) 115–123

ADONIS 000527289100085S

BBABIO 43354

Infrared spectroscopic signals arising from ligand binding and conformational changes in the catalytic cycle of sarcoplasmic reticulum calcium ATPase

Andreas Barth, Werner Mäntele and Werner Kreutz

Institut für Biophysik und Strahlenbiologie der Universität Freiburg, Freiburg (F.R.G.)

(Received 16 October 1990)

Key words: ATPase, Ca^{2+}-; Sarcoplasmic reticulum; Protein conformation; FTIR; ATP, caged

Fourier transform infrared spectroscopy was used to investigate ligand binding and conformational changes in the Ca^{2+}-ATPase of sarcoplasmic reticulum during the catalytic cycle. The ATPase reaction was started in the infrared sample by release of ATP from the inactive, photolabile ATP derivative P^3-1-(2-nitro)phenylethyladenosine 5′-triphosphate (caged ATP). Absorption spectroscopy in the visible spectral region using the Ca^{2+}-sensitive dye Antipyrylazo III ensured that the infrared samples were able to transport Ca^{2+} in spite of their low water content, which is required for mid-infrared measurements (1800–950 cm^{-1}). Small, but characteristic and highly reproducible infrared absorbance changes were observed upon ATP release. These infrared absorbance changes exhibit different kinetic properties. Comparison with model compound infrared spectra indicates that they are related to photolysis of caged ATP, hydrolysis of ATP in consequence of ATPase activity and to molecular changes in the active ATPase. The absorbance changes due to alterations in the ATPase were observed mainly in the region of Amide I and Amide II protein absorbance and presumably reflect the molecular processes upon phosphoenzyme formation. Since the absorbance changes were small compared to the overall ATPase absorbance, no major rearrangement of ATPase conformation as the result of catalysis could be detected.

Introduction

Ca^{2+}-transport from the cytoplasm of muscle cells into SR, necessary for muscle relaxation, is performed by the Ca^{2+}-ATPase of SR, an intrinsic membrane protein of about 110 kDa molecular mass. The energy required for this active transport process is provided by hydrolysis of ATP (for reviews see Refs. 1–6).

The transport mechanism involves several reaction steps, which are presumed to be accompanied by conformational changes, including a change between two major conformations, E_1 and E_2, having different chemical properties: E_1 is characterized by high-affinity Ca^{2+}-binding sites facing the cytoplasm; it is phosphorylated by ATP but not by P_i and can be dephosphorylated by ADP (ADP-sensitive phosphoenzyme) under formation of ATP. E_2 binds Ca^{2+} with low affinity from the inside of SR; it can be phosphorylated by P_i but not by ATP and cannot be dephosphorylated by ADP (ADP-insensitive phosphoenzyme) [7]. Although this model accounts for many of the observed results, some objections have been made [8–11]. The ATPase reaction scheme proposed by de Meis and Vianna [12] is shown in a simplified form in Fig. 1.

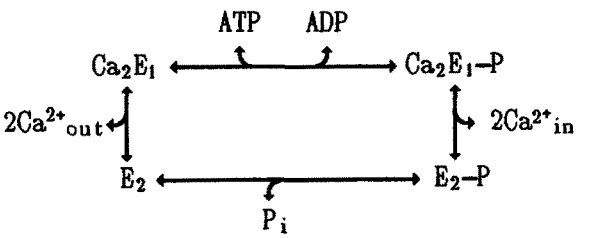

Fig. 1. Simplified reaction scheme of the Ca^{2+}-ATPase according to Ref. 12.

Abbreviations: SR, sarcoplasmic reticulum; Ca^{2+}-ATPase, Ca^{2+}-transporting ATPase (EC 3.6.1.38); caged ATP, P^3-1-(2-nitro)phenylethyladenosine 5′-triphosphate; FTIR, Fourier transform infrared; FITC, fluorescein 5′-isothiocyanate; EGTA, [ethyleneglycobis(oxyethylenenitrilo)]tetraacetic acid.

Correspondence: W. Mäntele, Institut für Biophysik und Strahlenbiologie, Universität Freiburg, Albertstr. 23, 7800 Freiburg, F.R.G.

Sequential binding of two calcium ions [13–15] from the cytoplasm to the high-affinity transport sites of E_1 enables the ATPase to react with ATP under formation of a phosphorylated enzyme intermediate, which occludes the bound Ca^{2+} from the cytoplasm [16–19]. The subsequent conversion of the phosphoenzyme from the ADP-sensitive (E_1P) to the ADP-insensitive form (E_2P) is accompanied by a decrease in Ca^{2+}-binding affinity [17,18,20] which leads to sequential Ca^{2+} release to the inside of the SR [9,13,19]. Hydrolytic cleavage of the phosphoenzyme [21] and rebinding of Ca^{2+} from the cytoplasm complete the reaction cycle [13,14,22]. Details of the transport mechanism, especially the coupling between ATP hydrolysis and active calcium transport, are still unknown.

The investigation of conformational changes in the catalytically active ATPase may help to elucidate this point. Of special interest is the E_1P–E_2P conversion, where Ca^{2+}-binding affinity and the reactivity towards ADP are changed. Several observations [23–26], including measurements of intrinsic fluorescence [8,27–31] or of attached fluorescent probes [32,33], indicate that there is a conformational change in connection with phosphoenzyme formation, which might reflect the E_1–E_2 transition [27,29,31–33]. However, there is experimental evidence that no major rearrangement of the ATPase occurs [34,35].

Infrared spectroscopy allows significant insight in the structure of small molecules. Changes in bond length, bond geometry, ligand binding and interaction with the environment reflect in the infrared spectrum, which therefore can be used for diagnostic purpose. Unfortunately, the analysis of proteins is hindered by a strong water absorbance and by the large size of proteins, leading to broad absorbance bands without detailed information. Recent analysis of the ATPase infrared absorption spectrum did not unambiguously detect differences between the E_1 and E_2 conformation [34,36,37]. Detailed information may be expected by subtracting the spectra of a protein prepared in two different states. However, this method involves uncertainties due to buffer subtraction and different sample concentration, which makes small changes in the spectrum difficult to detect. Previous work on retinal proteins [38,39], on the photosynthetic bacterial reaction centre [40] and on cytochrome *c* [41] showed that infrared spectroscopy is a powerful tool to investigate molecular changes, even at the level of individual bonds in a protein, provided that it is possible to start a protein reaction in the infrared cell. This concept of 'reaction-modulated infrared difference spectroscopy' avoids the above-mentioned uncertainties of spectrum subtraction and thus allows a more sensitive comparison of different enzyme states. While light flashes or the application of an electrochemical potential were used to trigger photoreactions or electron transfer reactions in the above-mentioned work, starting a protein reaction by simply mixing the substrate to the sample in a stopped flow apparatus is extremely difficult. This is due to the sample thickness of 10 μm and less, which is dictated by the strong absorbance of the scissor vibration of water around 1650 cm^{-1} [42]. In order to circumvent this problem, we use here the photolytic release of ATP from caged ATP to start the reaction cycle of the ATPase. Caged ATP is an inactive, photolabile ATP-derivative that releases ATP upon ultraviolet illumination [43,44].

In this work, we use ATPase samples prepared at low water content for infrared spectroscopy, but with retained Ca^{2+}-transport activity as determined by the use of the Ca^{2+}-concentration sensitive dye Antipyrylazo III [45–47]. Upon release of ATP from caged ATP, infrared absorbance changes were observed which were related to ligand binding and protein conformational dynamics, to ATPase hydrolysis activity and to the release of ATP.

Materials and Methods

ATPase preparation. Ca^{2+}-ATPase from rabbit hind leg and back muscle was prepared in the laboratory of W. Hasselbach according to the method of Hasselbach and Makinose (described in Ref. 48). It was stored at $-20\,°C$, after adding sucrose to give a final concentration of 0.3 M.

Sample preparation for infrared spectroscopy. Following thawing, ATPase was dialyzed overnight in a buffer containing 20 mM Mops/Tris (pH 6.8), 10 mM KCl, 800 μM $MgCl_2$ and 8 μM $CaCl_2$. Thin semihydrated films of SR vesicles were prepared by drying a solution of vesicles onto a CaF_2 window in a stream of nitrogen. Gravimetric controlled drying was stopped when the weight of the sample reached about 1.5 mg. The infrared cell was then closed with a second CaF_2 window which was separated from the first one by a 6 μm spacer. 'Normal' ATPase samples contained 100–150 μg protein, 300 nmol Mops/Tris (pH 6.8), 150 nmol KCl, 12 nmol $MgCl_2$, 0.12 nmol $CaCl_2$ in addition to the Ca^{2+} bound by the SR, 15 nmol caged ATP, 0.1 nmol Ca^{2+}-ionophore A23187 and 10 nmol glutathione. The sample volume was approx. 1 μl. In the case of Ca^{2+} transport measurements, the samples contained in addition 20 nmol Antipyrylazo III, but no ionophore A23187. Photolysis of caged ATP was investigated with samples of 'normal' sample composition, but with 45 nmol caged ATP, and without protein. Caged ADP samples were prepared by replacing caged ATP by 24 nmol caged ADP and 10 pmol adenylate kinase inhibitor, P^1,P^5-di(adenosine-5′) pentaphosphate [49]. For the FITC samples, 100–150 μg dialysed ATPase was incubated with 10 nmol of FITC at room temperature

for at least 2 h before drying [50,51]. For the 'Ca^{2+}-free' samples, 20 nmol EGTA were added before drying.

H_2O–^2H_2O exchange. For the deuterated samples, free water was removed almost completely. Then 1 μl ^2H_2O was added and mixed with the sample. The sample was closed with the second CaF_2 window and H–^{2}H exchange was allowed to take place for 6 h at room temperature. This preparations still contained a small amount of H_2O (< 5%).

Estimation of protein content of the samples. Protein content of the samples was estimated from the Amide I or II protein infrared absorbance bands. The absorbance was calibrated with completely dried samples, which were prepared from a solution of known protein content tested with the Coomassie blue test [57]. For samples in H_2O the Amide II absorbance difference between 1544 cm^{-1} and 1490 cm^{-1} was used, for samples in ^2H_2O the Amide I absorbance difference between 1710 cm^{-1} and 1654 cm^{-1}. This procedure gave only an upper limit of protein content for the ^2H_2O samples due to the superposition of a small amount of residual H_2O absorbance.

Photolysis of caged ATP. Photolysis of caged ATP was triggered by a xenon flash tube, which produced a flash energy of approx. 150 mJ in the spectral range from 305 nm to 424 nm at the area of the sample. A Schott UG11 filter was used to block the flashlight in the infrared. This setup produced a photolysis yield of up to 27% (for details see results).

FTIR measurements. FTIR measurements were performed with a Bruker IFS 25 instrument equipped with a HgCdTe detector of selected sensitivity in the following way: 15 subsequent single beam spectra (I_n, $n = 1,\ldots,15$) of the sample were recorded in the range from 1800 cm^{-1} to 950 cm^{-1}. Between the second and third spectrum the photolysis flash was applied. For all spectra 20 scans in 15 s were collected except for spectrum I_2, which was computed from 100 scans. All spectra were recorded with a resolution of 4 cm^{-1} and triangular apodization. The absorbance difference between spectrum I_2, immediately before the flash, and spectrum I_n, was obtained by calculating $D_n = -\log(I_n/I_2)$. This is a more direct expression for the difference spectrum than subtraction of the respective sample absorbance spectra. The first difference spectrum, D_1, calculated from spectra recorded before the flash, served as baseline control. The other showed the absorbance changes after application of the flash.

Model spectra for ATP hydrolysis. Model substances were aqueous solutions of 100 mM ATP and 100 mM (ADP + P_i). Both solutions were adjusted with KOH to pH 6.8. 4 μl of solution were placed without spacer between two CaF_2 windows and infrared absorbance spectra were recorded. After subtraction of CaF_2 absorbance the spectra were multiplied with an appropriate constant to give the same water absorbance at 2125 cm^{-1} (combination of scissor and torsion vibration or overtone of the torsion vibration [42]) as a water sample recorded under the same conditions. Then the water spectrum was subtracted. This procedure automatically ensured correction for different sample thicknesses.

Measurements of Ca^{2+} transport. Ca^{2+} transport was tested by measuring the absorbance change of the Ca^{2+}-sensitive dye Antipyrylazo III after release of ATP from caged ATP. Analogous to the FTIR measurements, 15 subsequent single-beam spectra in the visible range from 500 nm to 800 nm were recorded every 15 s with a rapid scan spectrophotometer built in our laboratory. Recording one spectrum needed 6 s. Between the second and third spectrum the photolysis flash was applied. Difference spectra were calculated in the same way as described above for the FTIR measurements.

Results

Control of Ca^{2+} transport activity of the samples with the Ca^{2+}-sensitive dye Antipyrylazo III

Antipyrylazo III has been shown to be a sensitive indicator of Ca^{2+} concentration changes suitable for the measurement of Ca^{2+} transport [45,46]. Changing the Ca^{2+} concentration induces characteristic changes in its absorbance of visible light. Since Antipyrylazo III does not penetrate the vesicles, it shows the Ca^{2+} concentration of the external medium, which is decreased during Ca^{2+} transport into the vesicles. We use this method as a control that the drying process during infrared sample preparation did not inactivate the ATPase. The full lines in Fig. 2 show changes of Antipyrylazo III absorbance which occurred at different times after ATP release in an ATPase infrared sample. The absorbance changes, first observed approx. 18 s after ATP release, reveal an absorbance decrease at 720 nm and 655 nm and a broad increase at 540 nm. The signals decay in the timescale of minutes (see spectra at 47 s, 75 s and 177 s). After several minutes, a small positive signal is detected. As seen by comparison with the Ca^{2+} titration (dotted line in Fig. 2), the difference spectra indicate a quick decrease of Ca^{2+} concentration upon ATP release which is followed by a slower return to the original concentration. The small positive signal observed several minutes after ATP release does not seem to be related to Ca^{2+} transport, because its shape is different from the Ca^{2+} titration spectrum. It is probably due to binding of other ions to the reaction products of caged ATP photolysis and ATP hydrolysis.

As a control, the Antipyrylazo III indicator measurements were repeated with caged ADP (dashed line in Fig. 2). The absorbance change upon ADP release is approximately twice as large as the signal upon ATP release, but does not show an absorbance change above 700 nm which is characteristic for Ca^{2+} concentration

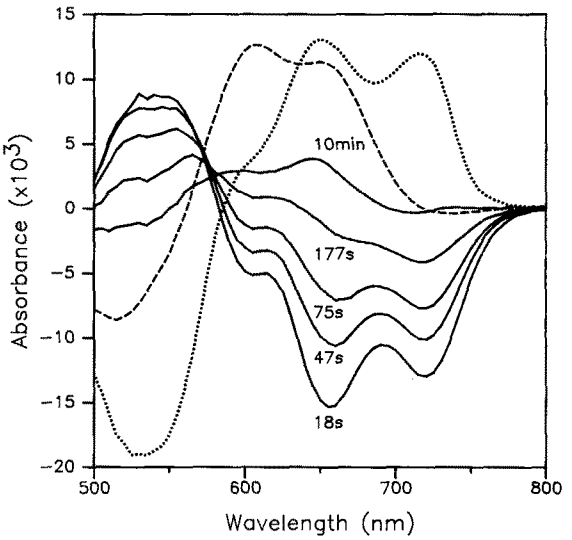

Fig. 2. Difference spectra of Antipyrylazo III absorbance. Full lines: Antipyrylazo III absorbance changes after ATP release in an ATPase sample (5 °C). The labels denote the mean time after ATP release at which the spectra were recorded. Dashed line: Antipyrylazo III absorbance changes after release of ADP in an ATPase sample (5 °C). The absorbance change is divided by 2. Dotted line: Absorbance change due to addition of 0.4 mM (final concentration) $CaCl_2$ to a buffer containing 200 mM Mops/Tris (pH 6.8), 100 mM KCl, 8 mM $MgCl_2$ and 80 μM $CaCl_2$. The absorbance change is divided by 2.

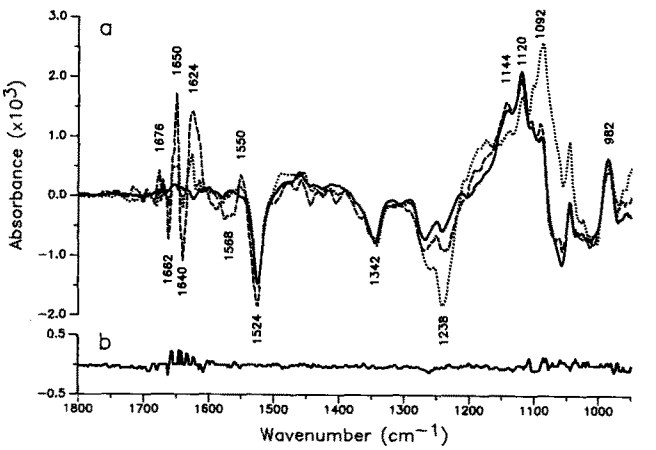

Fig. 3. Change of infrared absorbance due to ATP release from caged ATP in samples with and without ATPase (0 °C). (a) Full line: Caged ATP sample without SR ATPase. Approx. 19 nmol ATP were released. The absorbance change was divided by 2.7. Dashed line and dotted line: ATPase sample (about 6.5 nmol ATP released). Dashed line: Spectrum recorded within the first 8 s after ATP release. Dotted line: Spectrum recorded 2 min after ATP release. The labels denote the peak positions of the dashed spectrum in cm^{-1}. (b) Baseline control spectrum of the ATPase sample before the flash.

changes [45]. Comparison with the Ca^{2+} titration (dotted line in Fig. 2) clearly demonstrates that no Ca^{2+} concentration changes take place upon ADP release. The ADP signal can be explained partly by binding of Mg^{2+} to the reaction products of caged ADP photolysis, since photolysis in buffers containing either Ca^{2+} or Mg^{2+} produces absorbance changes characteristic for a concentration decrease of the salt present in solution (data not shown).

The ATP-driven Ca^{2+} uptake into SR vesicles indicates the functional integrity of the ATPase at a water content sufficiently low for infrared measurements in the mid-infrared range (1800–950 cm^{-1}).

Infrared absorbance changes of an ATPase sample upon ATP release from caged ATP

When ATP is released from caged ATP in an ATPase sample, the infrared absorbance in the region from 1800 cm^{-1} to 950 cm^{-1} exhibits characteristic and highly reproducible changes having different kinetic properties. The dashed and dotted line in Fig. 3 show difference spectra at about 8 s and 2 min after ATP release (recorded at 0 °C). According to their kinetic properties, three kinds of absorbance change can be distinguished:

(a) permanent changes that appear in the first spectrum (dashed line in Fig. 3) within 8 s after ATP release and are still present 2 min later (1524, 1342, 1270–950 cm^{-1});

(b) changes between 1300 cm^{-1} and 1000 cm^{-1} which rise more slowly on the time scale from several seconds to minutes, depending on temperature and sample composition; and

(c) transient changes between 1750 cm^{-1} and 1520 cm^{-1} appearing immediately after ATP release and decreasing when the slow change comes to its end.

Fig. 3b shows the baseline control spectrum which was recorded before ATP release as a control of the noise level. It is evident that the noise level is much lower than the size of the signals. This is a prerequisite for the high reproducibility of the signals.

It appears reasonable to assume that the different types of absorbance change reflect the molecular processes of caged ATP photolysis, ATP binding and hydrolysis, and conformational dynamics of the ATPase associated with its catalytic activity. In order to assign the absorbance changes, we investigated the photolysis of caged ATP and hydrolysis of ATP separately.

Infrared absorbance changes due to photolysis of caged ATP

Photolysis of caged ATP (Fig. 4) is accompanied by modification of several chemical groups of the molecule [44]. The NO_2 group converts to a NO group, a C=O bond is formed while two bonds are cleaved: a C–H bond and the C–O bond, that links the nitrobenzyl moiety to the γ-phosphate of ATP. These modifications

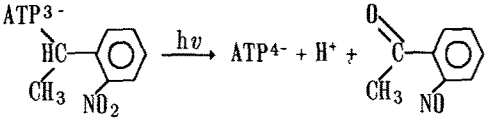

Fig. 4. Photolysis of caged ATP [44].

should reflect in the infrared difference spectrum between caged ATP and its photolysis products. The full line in Fig. 3 shows absorbance changes upon photolysis of caged ATP in a caged ATP sample containing no SR vesicles. They were obtained after release of approx. 19 nmol ATP and were multiplied with an appropriate constant to fit with the 1524 cm^{-1} and 1342 cm^{-1} peaks of the ATPase difference spectrum observed 2 min after ATP release (dotted line in Fig. 3). The absorbance changes appeared instantly and did not reveal kinetic components comparable to the slow and transient absorbance changes of the ATPase sample (dashed and dotted line in Fig. 3). We assign the minima at 1524 cm^{-1} and 1342 cm^{-1} to the asymmetrical and symmetrical stretching vibrations of the nitro group of caged ATP, which disappears during photolysis (see absorbance of nitrobenzyl compounds in Ref. 52). The bonds below 1270 cm^{-1} we attribute to a diminution of P–O double-bond character in the γ-phosphate, and presumably to the breaking of a C–O bond. If glutathione is omitted from the sample, an additional peak appears at 1684 cm^{-1} (data not shown), which is probably due to formation of the keto group in consequence of photolysis (see absorbance of benzoic acid compounds in Ref. 52). We would like to emphasize that no remarkable absorbance changes appear in the region between 1800 cm^{-1} and 1550 cm^{-1} in the caged ATP model sample.

The 1342 cm^{-1} and 1524 cm^{-1} absorbance differences due to caged ATP photolysis were used to estimate the efficiency of photolysis. These absorbance differences between two subsequent flashes decreased exponentially with the flash number (data not shown). From this exponential decrease a photolysis yield of up to 27% was calculated. The absorbance differences were in return used to calculate the amount of released ATP.

By comparing the absorbance changes of the caged ATP sample (full line in Fig. 3) with those of the ATPase sample (dashed and dotted line in Fig. 3), it is evident that the permanent absorbance changes of the ATPase sample (1524, 1342, 1270–950 cm^{-1}) can be attributed to photolysis of caged ATP.

Infrared absorbance changes due to hydrolysis of ATP

In order to investigate the absorbance changes generated by hydrolysis of ATP, we measured the absorbance spectra of the model substances ATP and (ADP + P_i) as described under Materials and Methods (full and dashed line in Fig. 5). We assign the absorbance maxima at around 1230 cm^{-1} to P–O vibrations that exhibit partial double-bond character and the one around 1100 cm^{-1} to P–O vibrations, having mainly single-bond character. The difference spectrum (ADP + P_i) minus (ATP) (named hydrolysis difference spectrum) shows a minimum at 1230 cm^{-1} and two maxima at 1170 cm^{-1} and 1080 cm^{-1} (dotted line in Fig. 5). The minimum at

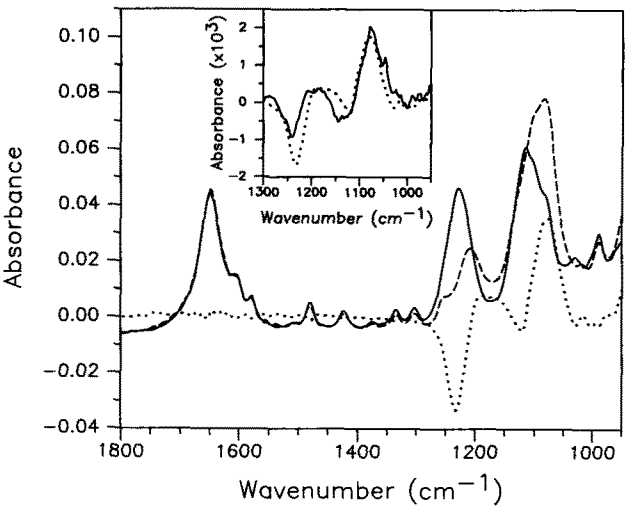

Fig. 5. Infrared absorbance and difference spectra of ATP and (ADP + P_i). Full line: Absorbance spectrum of 100 mM ATP, pH 6.8. Dashed line: Absorbance spectrum of 100 mM (ADP + P_i), pH 6.8. Dotted line: Hydrolysis difference spectrum, (ADP + P_i) absorbance minus ATP absorbance. Inset: Comparison of hydrolysis difference spectrum and slow absorbance change of the ATPase sample. Full line: ATPase difference spectrum recorded 2 min after ATP release minus the spectrum recorded immediately after ATP release. Dotted line: (ADP + P_i) absorbance minus ATP absorbance.

1230 cm^{-1} is observed because the number of P–O vibrations of partial double-bond character in (ADP + P_i) is less than in ATP. In contrast, the number of P–O vibrations of mainly single-bond character is greater, which explains the maximum at 1080 cm^{-1}. No absorbance difference is observed in the region from 1800 cm^{-1} to 1300 cm^{-1}.

A comparison between the hydrolysis difference spectrum and the slow absorbance changes of the ATPase sample is made in the inset of Fig. 5. The dotted line shows the hydrolysis difference spectrum in the region from 1300 cm^{-1} to 950 cm^{-1}, the full line the slow absorbance change of the ATPase sample. From the good agreement of the two difference spectra we conclude that the slow absorbance changes between 1300 cm^{-1} and 1000 cm^{-1} of the ATPase sample are due predominantly to hydrolysis of ATP.

Measurement of ATPase activity in infrared samples

Since infrared samples require a low water content, it is important to ensure that the ATPase samples catalyse ATP hydrolysis and Ca^{2+} transport. While the measurements with Antipyrylazo III prove the capability of the ATPase to transport Ca^{2+}, the hydrolysis absorbance changes in the infrared enable us directly to quantify the ATP hydrolysis activity of ATPase infrared samples. The absorbance change at 1238 cm^{-1} was used to measure the activity. Typical sample activities were about 0.25 μmol/min per mg protein for the first 20 s at 5 °C. Since complete removal of free water and subsequent rehydration decreased the sample activity

only slightly, we conclude that the drying process did not impair the functional properties of the ATPase. Contaminations of basic ATPase in our ATPase preparations could not account for the hydrolysis activity, since the same activity was observed in the presence of approx. 5 mM oxalate, which is known to inhibit basic ATPase [53].

Infrared absorbance changes due to molecular changes in the ATPase

From the investigation of the absorbance changes due to photolysis and hydrolysis, it is evident that the transient absorbance changes in the region from 1800 cm^{-1} to 1520 cm^{-1} cannot be explained by these reactions. It is suggestive to assume that these changes are caused by molecular processes in the ATPase during the catalysis of Ca^{2+} transport. In order to prove this hypothesis, several control samples were investigated including FITC-modified and EGTA-treated ATPase and samples with caged ADP instead of caged ATP. Modification of the ATPase with FITC blocks the nucleotide binding site of the ATPase and results in inhibition of ATPase activity [50,51]. EGTA also causes inhibition of Ca^{2+}-ATPase activity by removing calcium from the high-affinity binding sites of the ATPase [15]. ADP binds to the Ca^{2+}-ATPase but cannot be hydrolyzed [1,2,54].

A comparison between the 'normal' ATPase sample and the control samples is made in Fig. 6. The full lines show absorbance changes in the region from 1800 cm^{-1} to 1500 cm^{-1} that occurred within 8 s after release of ATP or ADP at 0 °C. The dotted lines show the baseline-control spectrum recorded before photolysis. The magnitude of the transient absorbance changes depended on the protein content of the samples and was therefore normalized to a typical protein content of 130 μg. The first difference spectrum after ATP release of the 'normal' ATPase sample (full line in Fig. 6a) shows maxima at 1676, 1650, 1624 and 1550 cm^{-1} and minima at 1662, 1640, 1568 and 1524 cm^{-1}. 2 min later the absorbance change has decreased significantly (dashed line in Fig. 6a) except for the minimum at 1524 cm^{-1}, which is due mainly to photolysis of caged ATP (full line in Fig. 3). However, the decrease of the peak amplitude at 1524 cm^{-1} within 2 min after ATP release reveals an additional protein contribution.

The transient absorbance changes of the 'normal' ATPase sample are not observed in control samples which contained 20 nmol EGTA (Fig. 6b), FITC modified ATPase (Fig. 6c) or samples in which ADP was released instead of ATP (Fig. 6d). However, they show a signal that rose slightly above the noise level and was significantly smaller than the signal produced by the 'normal' ATPase sample. This signal may be due to nucleotide binding to the ATPase in case of the caged ADP and the EGTA sample. None of the control sam-

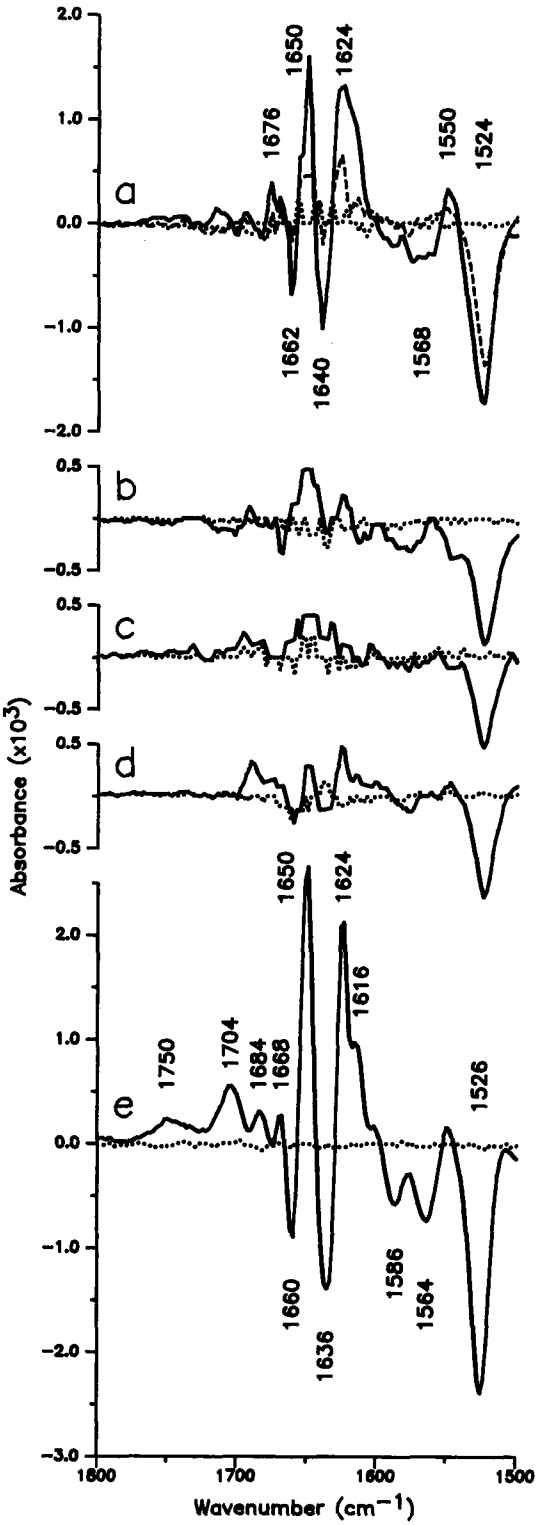

Fig. 6. Infrared absorbance change of ATPase samples in consequence of ATP or ADP release (0 °C). (a) 'Normal' ATPase sample, ATP release. (b) ATPase sample containing 20 nmol EGTA, ATP release. (c) FITC-modified ATPase, ATP release. (d) Release of caged ADP in an ATPase sample. (e) ATPase in ^2H_2O medium, ATP release. (a)–(e) Full lines: Absorbance difference recorded within the first 8 s after ATP or ADP release. Dashed line: absorbance change recorded 2 min after release of ATP. Dotted lines: baseline control spectrum recorded before ATP or ADP release. The labels denote the peak positions of the full-line spectra in cm^{-1}.

ples showed absorbance changes comparable to the 'normal' ATPase sample. Thus, we conclude that the observed transient absorbance changes in the region between 1750 cm^{-1} and 1520 cm^{-1} are due to molecular changes in the ATPase as a consequence of catalytic activity.

Replacement of H_2O by ^2H_2O and thus H–^{2}H exchange resulted in the difference spectrum shown in Fig. 6e. Compared to the ATPase sample in H_2O, new bands and intensity changes of several bands are observed. First, the overall absorbance change is increased in ^2H_2O. In addition, new maxima appear at 1750, 1704 and 1684 cm^{-1}. The shoulder of the 1624 cm^{-1} maximum (at approx. 1616 cm^{-1}) and the 1550 cm^{-1} peak are decreased. The activity of the samples in ^2H_2O, as determined by monitoring the band at 1238 cm^{-1}, was lower by a factor of about 2 than in H_2O. This is probably due to the effect of ^2H_2O on the overall turnover rate. For that reason it is not clear whether the spectral differences are due to H–^{2}H exchange or to accumulation of the ATPase in a different equilibrium of states in the catalytic cycle.

Discussion

Recent FTIR investigations analysed the secondary structure of ATPase samples that were prepared in the Ca_2E_1 and in an E_2P-like state using Fourier deconvolution and derivative techniques [34,36,37]. Arrondo et al. [37] found several differences in the composition of the E_2P infrared bands compared with the Ca_2E_1 bands, which he related to an additional α-helical structure (1650 cm^{-1}), missing of a β-sheet or turn structure (1677 cm^{-1}), protection against H–^{2}H exchange (1537 cm^{-1}) and to a different influence of the protein on the absorbance of the ester carbonyl groups of phospholipids (1760–1700 cm^{-1}). However, these differences could not be confirmed by other groups in the range of 1760–1700, 1565–1535 [36] and 1700–1600 cm^{-1} [34].

Release of ATP from caged ATP in an SR sample results in small but highly reproducible changes of infrared absorbance. We assign them to photolysis of caged ATP (mainly in the 1540–950 cm^{-1} region), hydrolysis of ATP in consequence of ATPase activity (mainly in the 1300–1000 cm^{-1} region) and to changes in the ATPase (mainly in the 1800–1520 cm^{-1} region) due to catalytic activity (Figs. 3 and 6). We claim that the method of starting a protein reaction in the infrared cell is a considerably more sensitive approach to detecting ligand binding and conformational changes than the method of comparing absorbance spectra of different samples. The use of the photo-chemo trigger presented here enables us to detect absorbance changes as small as 0.1% of total protein absorbance in the Amide I protein absorbance region.

During steady-state activity under optimal conditions, the active ATPase proteins accumulate to nearly 100% in the phosphorylated intermediate. A typical value for the maximal amount of phosphoenzyme is 4–5 nmol/mg protein. This number is usually accepted as the number of active sites, since it is half the number of Ca^{2+} high-affinity binding sites [4,6,13,18,29,31,55]. In addition, under conditions most closely related to our experiments, several groups found that 75–90% of phosphoenzyme are in the E_1P form [18,55,56]. Thus we conclude that the observed infrared protein absorbance changes reflect mainly the difference of infrared absorbance between the Ca_2E_1 and the Ca_2E_1P state. However, the small fraction of the enzyme in the E_2P state will also contribute to the signals.

The changes in infrared protein absorbance we observed are small compared to the total protein absorbance. The ratio between the peak-to-peak absorbance change and the total absorbance of active ATPase in the Amide I region was calculated to be only 1–2% (based on an amount of 4 nmol phosphoenzyme/mg SR protein and the molecular mass of 110 kDa). However, since the amount of phosphoenzyme could not be measured in our samples, it may be lower than estimated and the value of 1–2% only a lower limit. The small alteration in infrared absorbance upon formation of the phosphoenzyme indicates again [34,35] that phosphorylation of the ATPase is not accompanied by a major rearrangement of its conformation.

At present, the molecular interpretation of the difference spectra is far from being complete. The main absorption peaks at 1660, 1650 and 1636 cm^{-1} are within the range of Amide I absorption of peptide carbonyls. In the 1550 cm^{-1} region, peak amplitudes are much smaller and most probably not caused by the Amide II absorption, since no drastic changes upon H–^{2}H exchange are observed. As for the Amide I differential signals, one might be tempted to follow the interpretation of Arrondo et al. [37], who interpreted an additional band at 1650 cm^{-1} in the E_2P state in terms of changes of the protein conformation in the course of the catalytic cycle. However, the small band size as well the highly structured band features rather favour localized structural modifications at or around the phosphorylation and the calcium binding site. This interpretation seems to be supported by only very small Amide II changes.

Part of the discrepancies between the band analysis of Arrondo et al. [37] and the spectra presented here may be due to the following: we detected differences in infrared absorbance between the Ca_2E_1 and, presumably, the Ca_2E_1P state, whereas Arrondo et al. compared the Ca_2E_1 state with an E_2P-like state.

Above 1700 cm^{-1}, two distinct positive bands are observed in the ^2H_2O spectrum (Fig. 6e), which are almost completely absent in the H_2O spectrum. As

discussed above, the reduced activity of the ATPase samples in ^2H_2O is not due to the drying and rehydration procedure, but rather to a kinetic isotope effect in the reaction cycle. These two bands at 1750 cm^{-1} and 1704 cm^{-1} are also observed in H_2O samples with approx. 20% dimethylsulfoxide (data not shown), a condition which favours the E_2P state by inhibiting phosphoenzyme hydrolysis [55,58,59]. We thus assume that these bands are characteristic for the enzyme state rather than being caused by isotopic substitution. According to their position they might be caused by protonated amino acid side-chain carboxyl groups, the lower-frequency group (1704 cm^{-1}) being strongly H-bonded, the higher-frequency group (1750 cm^{-1}) being well-protected from intermolecular interactions. This assignment is supported by an isotopic shift of the band at 1704 cm^{-1} (^2H_2O) which is observed at 1710 cm^{-1} in H_2O with 20% dimethylsulfoxide (data not shown). For the extremely broad band at higher frequency (1750 cm^{-1}), an $H-^2H$ isotopic shift (estimated to be approx. -10 cm^{-1} [38]) is difficult to detect. Arrondo et al. [37] attributed band structures in this region to changes of protein–lipid interaction between the E_1 and E_2 state. The absence of a band at 1730 cm^{-1} (the maximum of phospholipid C=O vibration) in our spectra, together with an isotopic shift, however, favour an assignment to aspartic or glutamic acid side-chain residues. The nature of these bands will be discussed in detail in a further paper.

Conclusions

In summary, it has been demonstrated that the photolysis of caged ATP represents an elegant trigger for 'reaction-modulated infrared spectroscopy', allowing the molecular processes in ATPases to be studied on a level of sensitivity which has in the past been reached only for proteins performing light-induced or redox-induced reactions. Furthermore, progress in the synthesis of other photolabile 'caged' substrate analogues will allow investigations of a wide range of enzymes, not only the class of ATPases. As for the example presented here, it is of great value that the photolysis reaction and hydrolysis of ATP due to catalytic activity do not produce changes in infrared absorbance in the Amide I region of protein absorbance. This facilitates the distinction of absorbance changes due to the photolysis and hydrolysis reaction from protein absorbance changes. A further assignment of the latter bands on the level of individual bonds will necessitate chemical modification of amino acid side-chain groups as well as site-directed mutagenesis. Further work will be needed to obtain higher accumulation of the E_2P state. In addition, it will be necessary to determine the exact fractions of the molecules in the E_1 and E_2 states in order to quantify the amount of conformational dynamics.

Acknowledgements

We would like to thank Prof. W. Hasselbach for kindly supplying us with Ca^{2+}-ATPase and for stimulating discussions, as well as Dr. R.S. Goody for making caged ADP available to us. We gratefully acknowledge Dr. D.A. Moss for the use of his computer programs and S. Chaudhuri for his technical assistance.

References

1 Hasselbach, W. (1981) in Membrane Transport (Bonting, S.L. and De Pont, J.J.H.H.M., eds.), pp. 183–208, Elsevier, Amsterdam.
2 Hasselbach, W. (1974) in The Enzymes (Boyer, P.D., ed.), pp. 431–467, Academic Press, New York.
3 Andersen, J.P. (1989) Biochim. Biophys. Acta 988, 47–72.
4 Inesi, G. and Kurzmack, M. (1984) in Biomembrane Structure and Function, Topics in Molecular and Structural Biology, Vol. 4 (Chapman, D., ed.), pp. 355–410, Verlag Chemie, Weinheim.
5 De Meis, L. (1988) Methods Enzymol. 157, 190–206.
6 Inesi, G. and De Meis, L. (1985) in The Enzymes of Biological Membranes, Volume 3 (Martonosi, A., ed.), pp. 157–191, Plenum Press, New York.
7 Carvalho, M., De Souza, D. and De Meis, L. (1976) J. Biol. Chem. 251, 3629–3636.
8 Dupont, Y., Guillain, F. and Lacapere, J.J. (1988) Methods Enzymol. 157, 206–219.
9 Khananshvili, D. and Jencks, W.P. (1988) Biochemistry 27, 2943–2952.
10 Stahl, N. and Jencks, W.P. (1987) Biochemistry 26, 7654–7667.
11 Dupont, Y. (1983) FEBS Lett. 161, 14–20.
12 De Meis, L. and Vianna, A. (1979) Annu. Rev. Biochem. 48, 275–292.
13 Inesi, G. (1987) J. Biol. Chem. 262, 16338–16342.
14 Dupont, Y. (1982) Biochim. Biophys. Acta 688, 75–87.
15 Petithory, J.R. and Jencks, W.P. (1988) Biochemistry 27, 5553–5564.
16 Kurzmack, M., Verjovski-Almeida, S. and Inesi, G. (1977) Biochem. Biophys. Res. Commun. 78, 772–776.
17 Takisawa, H. and Makinose, M. (1983) J. Biol. Chem. 258, 2986–2992.
18 Nakamura, Y. and Tonomura, Y. (1982) J. Biochem. 91, 449–461.
19 Nakamura, J. (1987) J. Biol. Chem. 262, 14492–14497.
20 Shigekawa, M. and Dougherty, J.P. (1978) J. Biol. Chem. 253, 1458–1464.
21 Makinose, M. (1973) FEBS Lett. 37, 140–143.
22 Dupont, Y. (1976) Biochem. Biophys. Res. Commun. 71, 544–550.
23 Murphy, A.J. (1978) J. Biol. Chem. 253, 385–389.
24 Andersen, J.P., Vilsen, B., Collins, J.H. and Jørgensen, P.L. (1986) J. Membr. Biol. 93, 85–92.
25 Andersen, J.P. and Jørgensen, P.L. (1985) J. Membr. Biol. 88, 187–198.
26 Ross, D.C. and McIntosh, D.B. (1987) J. Biol. Chem. 262, 12977–12983.
27 Champeil, P., Le Maire, M., Møller, J.V., Riollet, S., Guillain, F. and Green, N.M. (1986) FEBS Lett. 206, 93–98.
28 Dupont, Y. and Leigh, J.B. (1978) Nature 273, 396–398.
29 Fernandez-Belda, F., Kurzmack, M. and Inesi, G. (1984) J. Biol. Chem. 259, 9687–9698.
30 Dupont, Y., Bennett, N. and Lacapere, J.-J. (1982) Ann. N.Y. Acad. Sci. 402, 569–572.
31 Andersen, J.P., Lassen, K. and Møller, J.V. (1985) J. Biol. Chem. 260, 371–380.
32 Obara, M., Suzuki, H. and Kanazawa, T. (1988) J. Biol. Chem. 263, 3690–3697.

33 Andersen, J.P., Jørgensen, P.L. and Møller, J.V. (1985) Proc. Natl. Acad. Sci. USA 82, 4573–4577.
34 Villalain, J., Gomez-Fernandez, J.C., Jackson, M. and Chapman, D. (1989) Biochim. Biophys. Acta 978, 305–312.
35 Csermely, P., Katopis, C., Wallace, B.A. and Martonosi, A. (1987) Biochem. J. 241, 663–669.
36 Buchet, R., Carrier, D., Wong, P.T.T., Jona, I. and Martonosi, A. (1990) Biochim. Biophys. Acta 1023, 107–118.
37 Arrondo, L.R., Mantsch, H.H., Mullner, N., Pikula, S. and Martonosi, A. (1987) J. Biol. Chem. 262, 9037–9043.
38 Siebert, F., Mäntele, W. and Kreutz, W. (1982) FEBS Lett. 141, 82–87.
39 Siebert, F., Mäntele, W. and Gerwert, K. (1983) Eur. J. Biochem. 136, 119–127.
40 Mäntele, W., Nabedryk, E., Tavitian, B.A., Kreutz, W. and Breton, J. (1985) FEBS Lett. 187, 227–232.
41 Moss, D., Nabedryk, E., Breton, J. and Mäntele, W. (1989) Biophys. J. 55, 394a.
42 Zundel, G. (1969) Hydration and Intermolecular Interaction, pp. 28–35, Academic Press, New York.
43 Kaplan, J.H., Forbush, III, B. and Hoffman, J.F. (1978) Biochemistry 17, 1929–1935.
44 McCray, J.A., Herbette, L., Kihara, T. and Trentham, D.R. (1980) Proc. Natl. Acad. Sci. USA 77, 7237–7241.
45 Scarpa, A. (1979) Methods Enzymol. 56, 301–338.
46 Scarpa, A., Brinley, F.J. and Dubyak, G. (1978) Biochemistry 17, 1378–1386.
47 Gilchrist, J.S.C., Katz, S. and Belcastro, A.N. (1990) Biochem. Biophys. Res. Commun. 168, 364–371.
48 De Meis, L. and Hasselbach, W. (1971) J. Biol. Chem. 246, 4759–4763.
49 Lienhard, G.E. and Secemski, I.I. (1973) J. Biol. Chem. 248, 1121–1123.
50 Highsmith, S. (1984) Biochem. Biophys. Res. Commun. 124, 183–189.
51 Pick, U. and Bassilian, S. (1981) FEBS Lett. 123, 127–130.
52 Szymanski, H.A. (ed.) (1963) Infrared Band Handbook, Plenum Press, New York.
53 Hasselbach, W. and Makinose, M. (1962) Biochem. Biophys. Res. Commun. 7, 132–136.
54 Meissner, G. (1973) Biochim. Biophys. Acta 298, 906–926.
55 Shigekawa, M., Wakabayashi, S. and Nakamura, H. (1983) J. Biol. Chem. 258, 14157–14161.
56 Shigekawa, M. and Dougherty, J.P. (1978) J. Biol. Chem. 253, 1451–1457.
57 Bio-Rad Laboratories (1977) Technical Bulletin No. 1051, Richmond, CA.
58 De Meis, L., Martins, O.B. and Alves, E.W. (1980) Biochemistry 19, 4253–4261.
59 The, R. and Hasselbach, W. (1977) Eur. J. Biochem. 74, 611–621.